

RATE OF ACTOMYOSIN ATP HYDROLYSIS DIMINISHES DURING ISOMETRIC CONTRACTION

N. A. Curtin, T. G. West, M. A. Ferenczi, Z.-H. He, Y.-B. Sun, M. Irving
and R. C. Woledge¹

INTRODUCTION

The aim of the experiments reported here was to measure the time course of ATP hydrolysis by actomyosin during isometric contraction. It is known from previous studies of energy produced as heat and work that most, but not all of this energy, is due to ATP hydrolysis stoichiometrically coupled to the creatine kinase reaction (Curtin and Woledge, 1979). Furthermore energy is produced at a much higher rate at the start of contraction than later. These facts raise the question of whether the rate of ATP hydrolysis by actomyosin, which is the major source of energy, changes during isometric contraction.

We have combined independent methods of measuring actomyosin ATP hydrolysis in our study of contracting dogfish fibres, and the results agree in showing that the rate of ATP hydrolysis by actomyosin declines substantially during contraction. This report extends our earlier accounts of the project (He et al., 1998; West et al., 2002).

¹ N.A. Curtin, T.G. West, M.A. Ferenczi, Imperial College London, Div. Biomed. Sci., BSF Section, Fleming Bldg., London SW7 2AZ, UK. Z-H. He, National Institute for Medical Research, The Ridgeway, Mill Hill, London NW7 1AA, UK. Y-B. Sun, M. Irving, King's College London, Sch. Biomed. Sci., New Hunt's House, Guy's Campus, London SE1 1UL, UK. R.C. Woledge, UCL Inst. Human Performance, Royal National Orthopaedic Hosp. Trust, Brockley Hill, Stanmore, Mddx. HA7 7LP, UK.

METHODS

Apparent Equilibrium Constant for Phosphate Binding to MDCC-PBP in Dogfish Fibres

One method we used was based on quantitating ATP hydrolysis from the change in fluorescence of MDCC-phosphate binding protein (MDCC-PBP) as it binds phosphate (He et al., 1997, 1999, 2000). The apparent equilibrium constant for the reaction is used to convert the fluorescence changes to amount of phosphate produced during contraction. We report here the apparent equilibrium constant measured in permeabilized white muscle fibres from the dogfish (*Scyliorhinus canicula*) under the conditions used in our experiments.

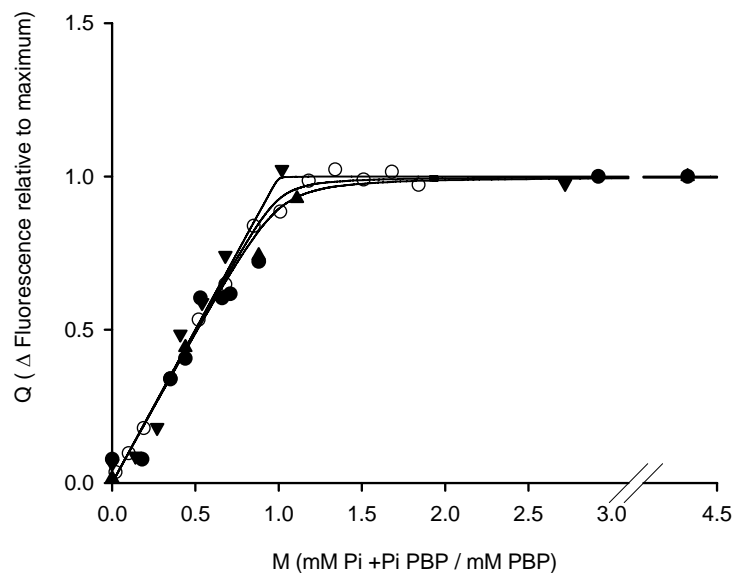


Figure 1. Fluorescence signal produced by known concentrations of phosphate and known concentrations of MDCC-PBP in permeabilized dogfish fibres (closed symbols) and rabbit fibres (open symbols). The lines show binding curves calculated for different dissociation constants and different the concentrations of MDCC-PBP. See text. Uppermost line: K_d 0.15 μM (as used by He et al. 1997) and MDCC-PBP 1.2 mM. Middle line: fitted apparent K_d 15.8 μM and MDCC-PBP 2.58 mM as used in the rabbit fibre experiments. Bottom line: fitted apparent K_d 15.8 μM and MDCC-PBP 1.2 mM as used in the dogfish fibre experiments.

Protocol

A series of loading solutions was prepared, as described below, containing 1.2 mM active MDCC-PBP and different known concentrations of phosphate in the range 0 to 4

mM. Permeabilized fibres were prepared and clips attached in the usual way. The sarcomere length was set to 2.1 – 2.2 μm before inducing rigor with the Ca^{2+} -free rigor solution. In each experiment the same permeabilized muscle fibre was immersed in each phosphate loading solution for 10 minutes before being transferred into silicone oil and the fluorescence signal measured.

Loading Phosphate solutions

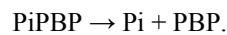
The zero-phosphate loading solution (200 mM ionic strength) contained (in mM) TES 60.00, MgCl_2 2.79, Ca^{2+} -EGTA 10.00, glutathione 10.00, K^+ -propionate 138.52, and MDCC-PBP 1.25. The 4 mM phosphate solution was made from the same constituents and ionic strength was held at 200 mM by modifying K^+ -propionate concentration to 130 mM. Solutions with intermediate phosphate concentrations were prepared by mixing the 0 and 4 mM phosphate solutions in appropriate proportion.

Evaluating the Apparent K_d for the Conditions used in these Experiments

The results of experiments on 3 dogfish fibres are shown in Fig. 1 along with the results from a rabbit fibre reported by He et al. (1997). Binding curves of the following form were fitted to the observed relationship:

$$Q = 0.5 (1 + M + D - (1 + 2M + M^2 + 2DM + 2D + D^2)^{0.5})$$

Where Q is the ratio of Δ fluorescence to maximum Δ fluorescence (where Δ fluorescence is the fluorescence minus the baseline value found by extrapolation to 0 Pi) all measured with fibre present. The value of Q is equivalent to the ratio PiPBP/C. C is the total concentration of phosphate binding protein (PiPBP + PBP, mM) used in the experiment expressed as the concentration of active phosphate binding sites. M is the ratio of the total concentration of phosphate (PiPBP + Pi, mM) in the loading solution to C (mM), and $D = \text{apparent } K_d / C$, and apparent K_d (units mM) is the apparent equilibrium constant for the reaction:



The best-fit value of apparent K_d was found by a least squares procedure using Excel Solver. For the experiments on dogfish and rabbit fibres, the best-fit value of apparent K_d was 15.8 μM . This value is larger than the value, 0.15 μM , used by He et al. (1997). However, both values represent relatively tight binding of phosphate by MDCC-PBP, which means that the most of the phosphate produced during contraction binds to MDCC-PBP and produces a fluorescence signal. We have corrected the records made during contraction using the apparent K_d 15.8 μM ; this correction amounted to an increase of 1.86% to the maximum rate of ATP hydrolysis, and a 14.2% increase to the total ATP hydrolysis during 0.5 s of contraction. The correction does not affect our interpretation of the results for ATP hydrolysis by actomyosin.

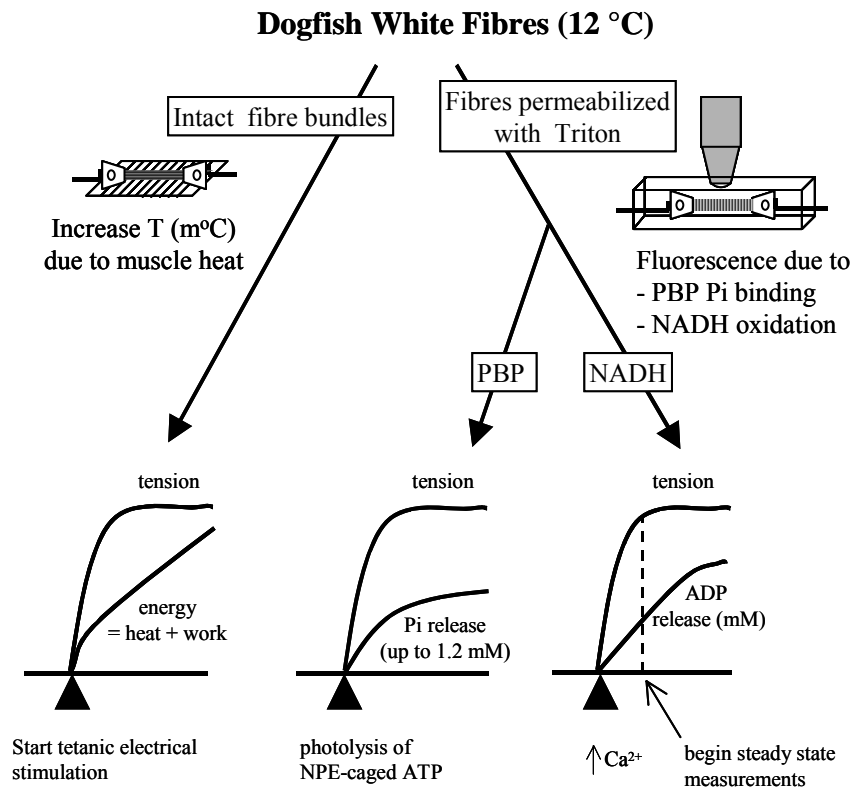


Figure 2. Diagram of the plan of the experiments to measure the energy produced and ATP hydrolysis by actomyosin in white fibres from dogfish. See text.

ATP Hydrolysis by Actomyosin

All experiments were done on white myotomal muscle fibres from the dogfish. Fibres were dissected in elasmobranch saline and all experiments were conducted at 12° C, normal body temperature for these animals. The plan of the experiments is shown diagrammatically in Fig. 2. Some fibre preparations were used “intact” and force and heat were recorded during electrical stimulation under isometric conditions. Other fibres were permeabilized with Triton and ATP hydrolysis by actomyosin during isometric contraction was measured from either fluorescence signal produced by phosphate binding to MDCC-PBP or by oxidation of NADH linked to ADP production.

Intact Fibres

For experiments on intact fibres the total energy output during contraction was measured as the sum of the heat production and mechanical work. Heat was detected by an antimony-bismuth thermopile as an increase in temperature. The mechanical work done against the series elasticity in these isometric (fixed end) contractions was evaluated from the force record and the stiffness of fibre preparation as described by Curtin et al. (1998). For all fibres the optimum stimulus strength and fibre length giving maximum isometric force (L_0) was determined at the start of the experiment. Fibre bundles were stimulated for 3.5s at a frequency of 50 Hz. In some cases the first 2 pulses were given at an interval of 10 ms. Heat loss correction was made in the usual way using the time constant for heat loss measured by the Peltier method (Woledge et al., 1985). Records were corrected for stimulus heat as described by Curtin and Woledge (1993).

The method of separating the energy due to actomyosin (AM) interaction from that due to other processes is described below.

Separating AM from non-AM energy turnover by intact fibres. To separate the energy produced by intact fibres into the part due to ATP hydrolysis by AM and the part due to other processes (ATP hydrolysis by sarcoplasmic reticulum- Ca^{2+} pump, Ca^{2+} -binding reactions, etc) we made use of the linear dependence of AM interaction on filament overlap at $L > L_0$ (see also Lou et al., 1997). In experiments on 9 fibres, force and energy production were measured during a 3.5s isometric (fixed-end) contraction at L_0 and at a length greater than L_0 . As expected, force “creep” occurred during the contractions at long length (Huxley and Peachey, 1961; Gordon et al., 1966a and b).

Background: what is force creep and how is it produced? Force creep is the gradual increase in force in a “fixed end” tetanus that continues after the initial rapid rise in force at the start of stimulation. It was described and characterized by Huxley and Peachey (1961) and Gordon et al. (1966a and b). Some important features are: it occurs at $L > L_0$ and is more obvious the longer the fibre length. Huxley and Peachey (1961) presented evidence showing that when a resting fibre is stretched to length $> L_0$, the end sarcomeres do not stretch as much as those in the centre of the fibre (direct observations of striations). When the fibre is stimulated force rises rapidly in the usual way as bridges attach in response to Ca^{2+} release from the sarcoplasmic reticulum and Ca^{2+} binding to troponin, etc. However, the force does not remain stabilized at a plateau

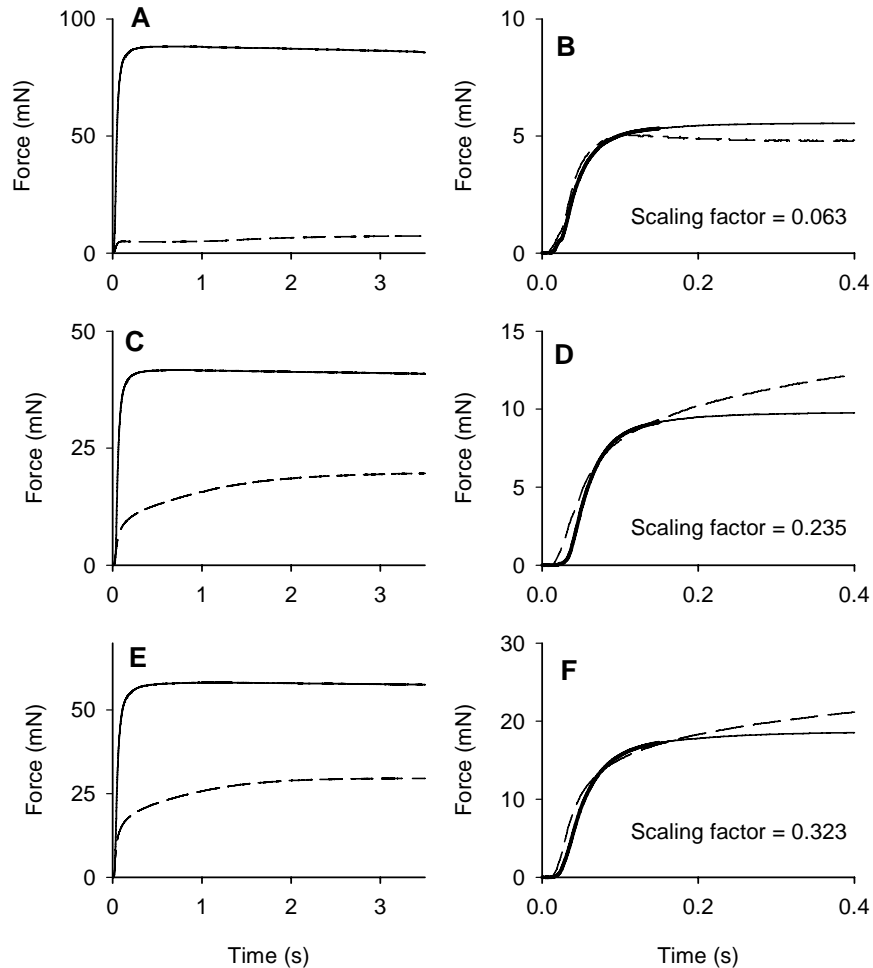


Figure 3. Records of force during isometric (fixed end) contractions by 3 intact fibre preparations. A, C and E show superimposed records for a contraction at L_0 (solid line) and at $L > L_0$ (broken line). B, D, and F show on an expanded scale the force recorded at $L > L_0$ (broken line) and the scaled version of the force recorded at L_0 (solid line). The scaling factor was chosen to give the best match to the force recorded at $L > L_0$. The thick solid line shows the part of the record (initial 150 ms) that was used to calculate the scaling factor (see text).

value, as it does in contractions at L_0 . Instead the force continues to increase or “creep” up gradually. Huxley and Peachey (1961) observed that the end sarcomeres, which have more overlap than those in the centre region, shorten at the expense of those in the centre.

Separating force creep from force that is proportional to filament overlap. In our experiments we need to separate creep force from the “normal” force because creep force represents crossbridge turnover and ATP hydrolysis that occurs **only** in the end sarcomeres, where we are not measuring energy output.

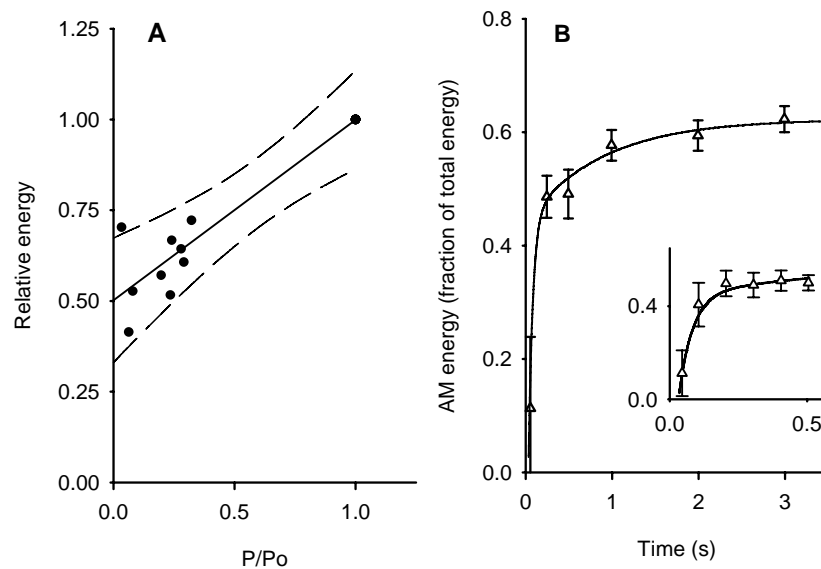


Figure 4 A. Example graph of energy output vs. force produced at different fibres lengths. Energy at each fibre length is expressed relative to that produced at Lo. Force corrected for creep (see text) is expressed relative to that produced at Lo. Energy output during 0.5 s contraction. Results for 9 fibre bundles. Solid line $y = 0.497(\pm\text{SEM } 0.037) x + 0.501(\pm\text{SEM } 0.027)$. The slope of this regression line, $0.497(\pm\text{SEM } 0.037)$, is the fraction of the energy due to AM. Broken line 95% confidence intervals. **B.** Variation of AM energy with time during isometric contraction. AM energy expressed as a fraction of the total energy output. Symbols are means \pm SEM for selected time points. Line is fitted through all time points (1point/ms). Inset shows values for early in the contraction on a larger time scale.

Our method of correcting force records for creep was based on the fact that creep develops gradually and progressively during a tetanus. In other words, the force at the beginning of the tetanus is least affected by it. Thus we have used only the force produced in the initial 150 ms of the contractions at $L > L_o$. Fig. 3 show pairs of records for contractions at L_o and at $L > L_o$ to illustrate the approach we used. For each fibre preparation the force recorded at L_o was scaled to fit that recorded from the same fibre preparation at $L > L_o$ using only the initial 150 ms of each contraction. The scaling factor was found using Excel Solver and was taken as the creep-free estimate of the force expressed as a fraction of the force produced at L_o (P/P_o in Fig. 4A); this fraction is also taken as the fraction of maximum filament overlap during the contraction.

Fig. 4A shows examples of the dependence of energy output on corrected force. The slope of the line is equivalent to the fraction of the energy output that is due to AM interaction. In this example the energy is that produced in the first 0.5 s of the contraction. Similar graphs were made for all the time points in the contraction; the slopes of these graphs plotted vs. time show how the fraction of energy turnover due to AM changed during the course of the contraction (see Fig. 4B).

Permeabilized fibres

For experiments on permeabilized fibres Triton was used to remove all membranes and thus prevent the ATPase activity due to membrane ion pumps. Methods used here are similar to those described previously by He et al. (1997, 1999, 2000) and Hilber et al. (2001). ATP hydrolysis in the initial 0.5 s of contraction was detected as the fluorescence change due to phosphate binding to phosphate binding protein (MDCC-PBP) after activation of contraction by flash photolysis of caged-ATP (He et al., 1997, 1999, 2000). ATP hydrolysis later in contraction after isometric force had reached its plateau value was detected as the fluorescence change due to NADH oxidation coupled to ADP production by AM ATP hydrolysis; in these experiments the fibre was activated by increasing Ca^{2+} (Hilber et al., 2001).

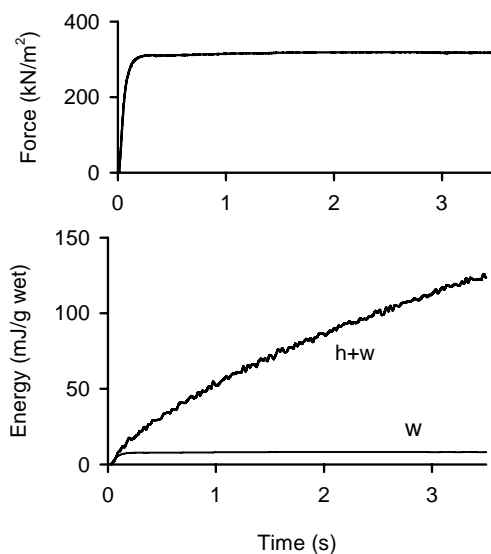


Figure 5. Example record of force (upper part) and energy (lower part) recorded during an isometric (fixed end) contraction of a bundle of intact fibres. Tetanus duration was 3.5s. The total energy is labelled h+w and the internal work against the series elasticity is labelled w.

Fixing fibre ends and attaching clips. During this project we developed a variation of the routine for fixing the ends of permeabilized fibre. In the usual routine a small bundle was dissected from the muscle slice and then permeabilized. The myosepta

(tendon sheets) at the ends of the bundle were removed at this stage so that a single fibre could be drawn out from the bundle. Aluminium T-shaped clips were loosely folded over each end and used to secure the fibre during fixation of the ends with glutaraldehyde. Clips were left relatively loose so that the fixative could reach the part of the fibre inside the clip. After fixation the clip was pinched tight.

In the revised protocol an intact single fibre was dissected and the myosepta were left intact at each end of the fibre. The myosepta were used, rather than T-clips, to support the fibre during the end-fixing process. Hence, fixative flowed directly over the surface of the fibre ends. After fixation, the myosepta were removed and the T-clips were folded firmly onto the fixed portion of the fibre ends. This modification was used for 3 of the 4 fibres used in the NADH experiments. It greatly improved our success with sustaining the Ca^{2+} -activated contractions for up to 20 s, and the fibres produced higher forces than those prepared by the usual fixation and clip routine.

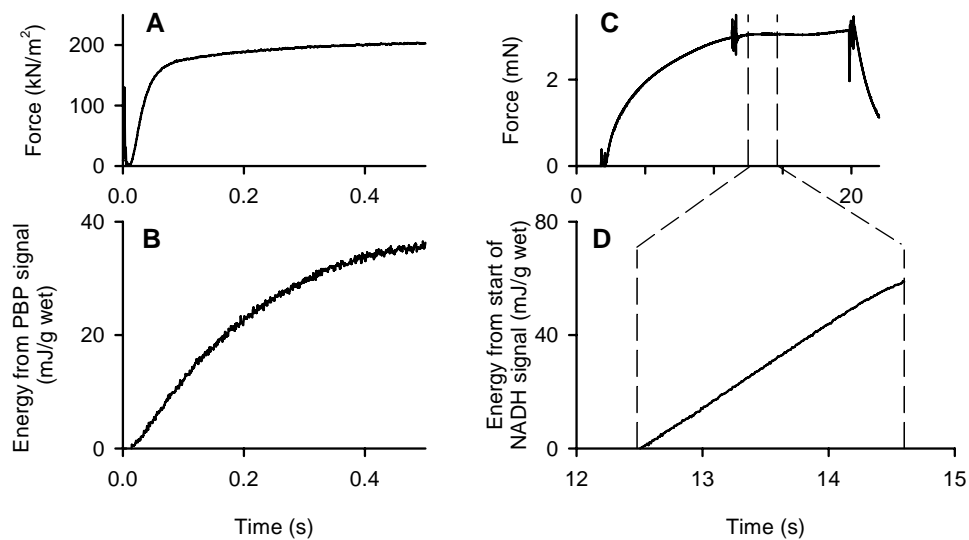


Figure 6. Records of force and energy from ATP hydrolysis by actomyosin in permeabilized fibres. **A** shows force and **B** shows the energy calculated from the MDCC-PBP signal during the initial 0.5 s of isometric contraction. **C** is the force record from an experiment using the NADH assay. The vertical broken lines mark the start and end of the period when NADH was measured. **D** shows the energy calculated from the change in NADH from its value at the start of the measurement, which corresponded to about 10s of contraction in this experiment. Note particularly the differences in scales in **B** and **D**.

Expressing ATP hydrolysis in energy units. Measured values of ATP hydrolysis were converted to energy units for comparison with the result from the intact fibres using the molar enthalpy for ATP hydrolysis coupled to the creatine kinase reaction, 34 kJ/mol ATP hydrolysis (Woledge et al., 1985), and assuming muscle density to be 1.06.

Normalizing for Size

Forces are expressed relative to cross sectional area to take account of variation in fibre size. Cross sectional area was measured as:

$$A = 4.9 w/d L$$

Where A is cross sectional area (mm^2), w is dry weight (mg). 4.9 is wet to dry weight ratio for white fibres from dogfish (Curtin and Woledge, 1993), d is density, which was assumed to be 1.06, and L is the length (mm) of the fibre at L_0 , the length given maximum isometric force.

RESULTS AND DISCUSSION

Figure 5 shows example records of force and energy output during a 3.5 s isometric tetanus of a bundle of intact fibres. The force increases rapidly to its plateau value and remains relatively constant after the first few hundred ms of stimulation. Energy is the sum of heat production and the “internal” work done against the series elasticity. Both the total energy (heat + internal work) and “internal” work are shown in Fig. 5. The energy output is fastest at the start of the contraction and the rate declines continuously. The energy output continues to decrease even after the fibres have stopped doing “internal” work.

We evaluated the amount of energy output due to actomyosin using the relationship shown in Fig. 4B which shows how the fraction of total energy due to actomyosin varied during contraction.

$$AM_t = f_t E_t$$

Where AM_t is the actomyosin energy at time t, f_t is the fraction at time t (see Fig. 4B and Methods) and E_t is the total energy output at time t (Fig. 5). Results for 17 fibre preparations were analysed in this way. The rate of energy output from actomyosin was calculated at various time points in the contraction. The mean values of the rates are shown in Fig. 7.

Figure 6 shows example records from two experiments on permeabilized fibres. The panels on the left show force and energy output detected during the initial 0.5 s of contraction. In these experiments, MDCC-PBP was used to monitor ATP hydrolysis by actomyosin. Contraction was initiated by photolysis of caged ATP at time 0. Phosphate production is not reported for the times after 0.5s of contraction for two reasons: the 1.2 mM MDCC-PBP present in the fibre becomes saturated with phosphate and therefore cannot report continuing ATP hydrolysis, and ATP supply becomes depleted.

Measured values of ATP hydrolysis were expressed in the equivalent energy units (see Methods). It is clear from Fig. 6B that energy production due to actomyosin ATP hydrolysis is fastest very early in the contraction, and the rate then declines. Rates were calculated at three time points and are shown in Fig. 7 (mean values from 15 experiments). The general pattern of a sharp decline in the rate matches that found in intact fibres.

As described in the Methods, we found that the apparent equilibrium constant for phosphate interaction with MDCC-PBP was somewhat different than the K_d used by He et al. (1997, 1999, 2000). To examine the influence of the value of the apparent equilibrium constant, we calculated the rates of ATP hydrolysis by our fibres using both values, and the results are shown in Fig. 7. The small open circles are for the tighter binding constant used by He et al. and the large open circles are for the binding constant reported here as measured in the presence of the permeabilized fibres. The maximum rates early in the contraction are hardly affected by the value of the apparent equilibrium constant. While the rate at 0.5 s is dependent on which equilibrium constant is used, in both cases the rate falls dramatically during the first 0.5 s of contraction.

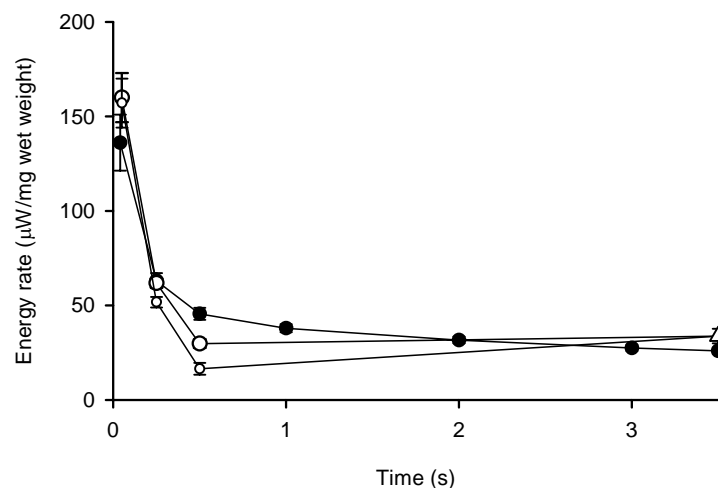


Figure 7. Energy rate during isometric contraction. Open symbols show energy rate due to ATP hydrolysis by actomyosin in permeabilized fibres detected with MDCC-PBP ($n=15$ fibres, apparent K_d 15.8 μM for large \circ , and K_d 0.15 μM for small \circ) and with NADH assay ($n=4$ fibres, Δ). Closed symbols show rate of energy release by actomyosin by intact fibres; energy release detected as heat and work ($n=17$ fibre preparations, \bullet). Mean \pm SEM.

Fig. 6B shows example records of force and energy output determined from the oxidation of NADH, which reports ADP formed during ATP hydrolysis by actomyosin in the skinned fibre. In these experiments the fibres were activated by increasing the Ca^{2+} and thus the rate of rise of force is less than in the other types of experiment. Once force had reached a plateau value, measurement of NADH oxidation commenced. The broken vertical lines in Fig. 6B and D mark the measurement period. The time course of energy release due to ATP hydrolysis is shown in Fig. 6D on an expanded time scale.

Clearly the rate is much lower at this time late in contraction than earlier. Note the difference in the time scales for Fig. 6B and D. It is also striking that the rate of energy release due to ATP hydrolysis by actomyosin is constant during this period in contrast to that earlier in contraction (Fig. 6B). Experiments of this type were done on 4 fibres and the mean result for the rate energy due to ATP hydrolysis by actomyosin late in contraction is shown in Fig. 7, plotted at nominal time 3.5 s. This rate is in good agreement with the rate at 0.5 s determined in the MDCC-PBP experiments.

CONCLUSIONS

The results in Fig. 7 show that the rate of energy output due to actomyosin alone as measured in intact fibres and in permeabilized fibres match well, and are in good agreement in showing that the rate is highest early in contraction and then declines dramatically. Our evidence indicates that the rate is relatively stable after the first 0.5 s of contraction.

At least part of the early high rate is due to internal work being done against the series elasticity as force rises. However, after force reaches its plateau value internal work ceases (Fig. 5). Thus it seems unlikely that internal work can completely explain the decline in ATP hydrolysis by actomyosin. As Fig. 7 shows the rate declines significantly between 0.25 and 0.5 s, a time when force is constant.

ACKNOWLEDGEMENTS

This work was supported by a grant from the Wellcome Trust.

REFERENCES

- Curtin, N.A., Gardner-Medwin, A.R. and Woledge, R.C. (1998). Predictions of the time-course of force and power output by dogfish white muscle fibres during brief tetani. *J. exp. Biol.* **201**: 103-114.
- Curtin, N.A. and Woledge, R.C. (1979). Chemical changes and energy production during contraction of frog muscle: How are their time courses related? *J. Physiol.* **288**: 353-366.
- Curtin, N.A. and Woledge, R.C. (1993). Efficiency of energy conversion during sinusoidal movement of white muscle fibres from the dogfish, *Scyliorhinus canicula*. *J. exp. Biol.* **183**: 137-147.
- Lou, F., Curtin, N.A. and Woledge, R.C. (1997). The energetic cost of activation of white muscle fibres from the dogfish, *Scyliorhinus canicula*. *J. exp. Biol.* **200**: 495-501.
- Gordon, A.M., Huxley, A.F. and Julian, F.J. (1966). Tension development in highly stretched vertebrate muscle fibres. *Journal of Physiology* **184**:143-169.
- Gordon, A.M., Huxley, A.F. and Julian, F.J. (1966). The variation in isometric tension with Sarcomere length in vertebrate muscle fibres. *Journal of Physiology* **184**:170-192.
- He, Z-H., Chillingworth, R.K., Brune, M., Corrie, J.E.T., Trentham, D.R., Webb, M.R. and Ferenczi, M.A. (1997). ATPase kinetics on activation of rabbit and frog permeabilized isometric muscle fibres: a real time phosphate assay. *Journal of Physiology* **501**, 125-148.
- He, Z-H., Chillingworth, R.K., Brune, M., Corrie, J.E.T., Webb, M.R. and Ferenczi, M.A. (1999). The efficiency of contraction in rabbit skeletal muscle fibres, determined from the rate of release of inorganic phosphate. *Journal of Physiology* **517**, 839-854.

- He, Z-H., Bottinelli, R., Pellegrino, M.A., Ferenczi, M.A. and Reggiani, C. (2000). ATP consumption and efficiency of human single muscle fibers with different myosin isoform composition. *Biophysical Journal* **79**, 945-961.
- He, Z-H., Ferenczi, M.A., Lou, F., Curtin N.A. and Woledge, R.C. (1998). A comparison of the energy turnover detected by heat production and by P_i assay in dogfish isolated muscle fibres. *J. Physiol.* **509**: 42P.
- Hilber, K., Sun, Y.-B., and Irving, M. (2001). Effects of sarcomere length and temperature on the rate of ATP utilisation by rabbit psoas muscle fibres. *Journal of Physiology* **531**, 771-780.
- Huxley, A.F. and Peachey, L.D. (1961). The maximum length for contraction in vertebrate striated muscle. *J. Physiol.* **156**: 150-165.
- West, T., Curtin, N.A., Ferenczi, M.A., He, H.-Z., Sun, Y.B., Irving, M., and Woledge, R.C. (2002). Quantifying isometric force-dependent energy release in white muscle by comparing contraction energetics in intact and skinned fibres. *J. Muscle Research and Cell Motility* **23**: 26-27.
- Woledge, R.C., Curtin, N.A. and Homsher, E. (1985). *Energetic Aspects of Muscle Contraction*. Monograph of the Physiological Society, No. 41, Academic Press, London.